2020 IEEE International Conference on Robotics and Automation (ICRA)
31 May - 31 August, 2020. Paris, France

Distributed Rotor-Based Vibration Suppression for Flexible Object Transport and Manipulation

Hyunsoo Yang[1], Min-Seong Kim[1], and Dongjun Lee[1]

***Abstract*— The RVM (Robot-based Vibration Suppression Modules) is proposed for the manipulation and transport of a large flexible object. Since the RVM is easily attachable/detachable to the object, this RVM allows distributing over the manipulated object so that it is scalable to the object size. The composition of the system is partly motivated by the MAGMaS (Multiple Aerial-Ground Manipulator System) [1]–[3], however, since the quadrotor usage is mechanically too complicated and its design is not optimized for manipulation, thus we overcome these limitations using distributed RVMs and newly developed theory. For this, we first provide a constrained optimization problem of RVM design with the minimum number of rotors, so that the feasible thrust force is maximized while it minimizes undesirable wrench and its own weight. Then, we derive the full dynamics and elucidate a controllability condition with multiple distributed RVMs and show that even if multiple, their structures turn out similar to [2] composed with a single quadrotor. We also elucidate the optimal placement of the RVM via the usage of controllability gramian which is not even alluded in [2] and established for the first time here. Experiments are performed to demonstrate the effectiveness of the proposed theory.**

I. Introduction

Large-size object transport and manipulation are one of the important tasks in industries, thus, these tasks also have been tried to be partially or fully handled by robotic systems typically in the assembly line in manufacturing. Regarding large-size object manipulation, there are several attempts to bring the robotic system to the outside of the factory using multiple robots [4]–[6]. Recently, ETHZ demonstrates a structure construction by assembling steel rebar, timber, and blocks using robotic manipulator [7]. ATOUN is proposed to assist human workers to transport a heavy object [8].

However, the above-mentioned results are limited in rigid object manipulation. On the other hand, these large-size objects often include long/slender object, such as bar, beam, and pipe. For this long/slender object handling, an induced torque by center-of-mass far from the grasping location is crucial as well as its high payload. As the length of the object gets longer, the deflection and the vibration become significant, thus it is hard to be handled by the conventional robotic system and possibly hazardous due to undesirable vibration.

In this paper, we propose a robot-based vibration suppression modules (RVM) which is optimally designed to manipulate the large flexible object while suppressing its vibration. Since the RVM is easily attachable/detachable to the object, an arbitrary number of the distributed RVMs can be adapted to various length/shape/weight of object. The system composition of the RVM is partly motivated by our previous result of MAGMaS (Multiple Aerial-Ground Manipulator System) [2], which utilizes a single quadrotor at the flexible load-tip. However, the quadrotor requires mechanically complicated and large payload structure, e.g., passive rotational joint, to connect the object while allowing free rotation. Besides, the quadrotor is optimized for flying capability in terms of the number of the rotors and its allocation [9]. The design and distributed actuation principles are partly inspired by ODAR (Omni-Directional Aerial Robot) [10] and LASDRA (Large-size Aerial Skeleton System with Distributed Rotor Actuation) [11], [12]. In these two results, the aerial robots are composed of distributed unit modules designed to maximize control wrench for omni-directional flying on each rigid link while the RVM is designed for vibration suppression of flexible object with a more simplified and compact design.

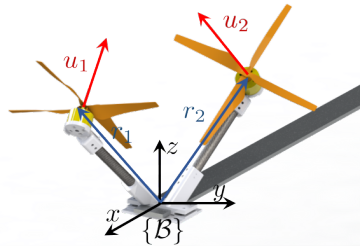

Fig. 1. Optimized design and rotor allocation of RVM.

We aim the role of the RVM as follows: 1) vibration suppression of the flexible load; and 2) object weight sharing to support limited ground manipulator torque. Therefore, we first provide a novel RVM design by optimizing the thrust generation along the sagittal plane while minimizing undesirable wrench along other directions based on contraiend optimization. Here, we utilize two rotors which is the minimum number that can generate control actuation along $E(2)$. Since an arbitrary number of the RVM can be utilized, we derive the system dynamics for arbitrary number of RVM and show that the flexible load dynamics is composed of linear diagonal matrices even with multi-modules. In the control problem, since the number of vibration modes and RVM can be arbitrary and this might induce controllability issue, thus we come up with controllability condition and elucidate its physical meaning for the distributed RVMs thanks to dynamic structure similar to [2]. Furthermore, we provide not only the place not to allocate the RVM based on controllability but also the place the RVM needs to be allocated to maximize vibration suppression capability based on controllability gramian. Experiments are performed to demonstrate the effectiveness of the proposed theory and RVM.

The rest of the paper is organized as follows, Sec. II explains how the RVM is optimally designed. In Sec. III, the dynamical model of the system including the vibrations in the load is derived and Sec. IV makes use of it to derive controllability and optimal placement. Sec. V presents experimental results which validate our approach, and Sec. VI highlights our conclusion and path for future works.

Research supported in part by the Basic Science Research Program (2015R1A2A1A15055616, 2020R1A2C3010039) and the Engineering Research Center Program (2016R1A5A1938472) of the National Research Foundation, MSIP, Korea; the Industrial Strategic Technology Development Program (10060070) of MOTIE, Korea;

[1] Department of Mechanical & Aerospace Engineering and IAMD, Seoul National University, Seoul, Republic of Korea. {yangssoo, mskim1143, djlee}@snu.ac.kr, Corresponding author: Dongjun Lee.

II. Robot-based Vibration Suppression Modules Design

A. System Description

We recall the composition of distributed RVMs and a ground manipulator for the flexible object manipulation. A manipulation system consists of a n-degrees of freedom (dof) ground manipulator, a load/object to be manipulated and distributed RVMs connected to the load, see Fig. 5. This system is proposed to overcome the limitation of approaches with quadrotor [1]–[3] by taking advantages of distributed modules with rotor actuation: 1) optimized design and simplified structure for manipulation and vibration suppression; and 2) dealing with large and flexible objects with distributed RVMs.

We assume a manipulated object as a long bar with skewed rectangular shape cross-section so that the transverse vibration is substantial only, while that along the others are negligible. We also confine ourselves to the case of planar manipulation for simplicity and the results are extendable to more general cases of course. We do not limit the location and the number of RVMs connected to the flexible load (c.f., one-quadrotor at the bar-end [2]). The RVM is rigidly connected to the flexible load through screw tightening mechanisms. This simple connection structure provides lighter and smaller RVM compared to a passive rotational joint in [2].

The actuation property of the rotor that generates both thrust force and moment along the rotor rotation axis makes the design problem non-trivial. Here, we consider to use the thrust force for vibration suppression control, then an undesirable torque can affect to other direction, e.g., a torsional torque. Therefore, we should consider both maximizations of thrust force in the sagittal plane and minimization of the torsional torque. Different from the conventional multirotor drone, the RVM does not necessary to have at least four rotors for flying capability, thus we utilize only two rotors for RVM which is sufficient to provide control input in $E(2)$ to minimize the number of rotors while realizing the compact and lightweight design.

B. Design Optimization

The goal of module design optimization is to specify the optimal attaching location of each rotor $r_i \in \Re^3$ and the respective thrust generation direction $u_i \in \Re^3$ all expressed in the RVM body frame $\mathcal{B}$. The search space of the optimization is then given by $\mathcal{U} := \{u_i \in \Re^3 | u_i^T u_i = 1, i = 1, 2\}$ and $\mathcal{R} := \{r_i \in \Re^3 || r_i| \leq r_{max}, i = 1, 2\}$ where $\mathcal{U}$ and $\mathcal{R}$ are the set of the thrust direction vectors and the location vectors, respectively, the condition $u_i^T u_i = 1$ is used to let $u_i \in S^2$, and r_{max} is the maximum allowable length for all the rotor locations. Here, we set $r_{max} = 0.15m$. Our design procedure presented here can also be extended for other numbers of rotors as well.

We can then formulate the design optimization problem as a constrained optimization problem s.t.

$$(u_1^*, u_2^*, r_1^*, r_2^*) := \arg \max_{u,r} \ (u_1 \times u_2)^T e_y \tag{1}$$

$$\text{subj. to } u_i^T u_i = 1, \quad r_i \in \mathcal{R} \tag{2}$$

$$(r_i \times u_i + \gamma u_i) \cdot e_x = 0, \quad \sum r_i \times e_z = 0 \tag{3}$$

$$\frac{|(r_1 - r_2) \cdot (u_1 \times u_2)|}{|u_1 \times u_2|} \geq d_{aero} \tag{4}$$

where $(\cdot)^*$ is optimal value, γ is thrust to moment ratio and $e_x, e_y, e_z \in \Re^3$ are unit vector of corresponding axis. The thrust generated by two rotors renders a plane whose normal vector is $u_1 \times u_2$ while its area is $|u_1 \times u_2|$. The bigger area means the bigger thrust generation capability along the plane. Therefore, to maximize thrust generation capability along xz-plane, we project this area into xz-plane for the cost function. Each constraints stand for following conditions: (2) constrain unit direction vector $u_i \in S^2$ and limit the maximum volume of the rotor location; (3) balance torsional torque around x-axis induced by rotor thrust and moment to prevent torsional deflection of the flexible load and balance torsional torque around x-axis induced by weight of the acutator; and (4) constrain the airflow interference among rotors by ensuring the distance among their airflow larger than a certain value d_{aero}. (4) represent the shortest distance between the center axis of the cylinder produced by airflow. As shown in [10], if the distance between two rotors is longer than a certain value d_{aero}, the airflow interference can be negligible. We solve this constrained optimization and the resultant RVM design is illustrated in Fig. 1.

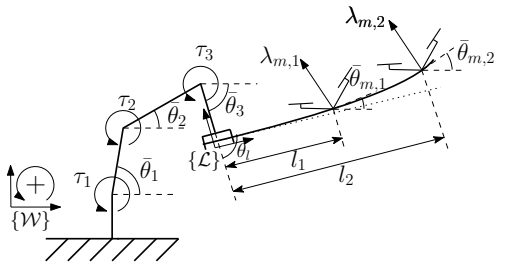

Fig. 2. Sketch of the configuration of the system.

III. Dynamics Modeling with Multiple Distributed RVMs

From the sketch in Fig. 2, we detail the notations used throughout the paper. On the ground, n-DoF robot arm is mounted whose joint configuration is defined as $\theta \in \Re^n$. The position of each joint, the center-of-mass of each links and end-effector of robot arm w.r.t. the inertial frame $\mathcal{W}$ are defined as $p_i^{\mathcal{W}} \in \Re^2$ and $p_{c,i}^{\mathcal{W}} \in \Re^2$ and $p_e^{\mathcal{W}} \in \Re^2$ respectively. For brevity, we will omit the $\mathcal{W}$ when the position is represented in the inertial frame. Define the position and the orientation of the RVM attached along the flexible load w.r.t. $\mathcal{W}$ as $p_{m,i} \in \Re^2$ and $\theta_{m,i} \in \Re$. For any angle, e.g. θ, the notation $\bar{\theta}$ represents the absolute angle, e.g., $\bar{\theta}_i = \sum_{j=1}^{i} \theta_j$, while θ representing relative angle throughout this paper.

The flexible load is rigidly attached to end-effector of the robot arm, thus relative angle between the end-effector and the flexible load is constant θ_l. As shown in Fig. 3, the position and orientation of the flexible load along the x-axis w.r.t. the flexible load frame $\mathcal{L}$ at time t can be written as $p_f^{\mathcal{L}}(x,t) = (x; w(x,t))$ and $\theta_f(x) = \frac{\partial w(x,t)}{\partial x}$ where $w(x,t)$ is the deflection along z-direction at x in $\mathcal{L}$. Recall that the RVMs are rigidly attached to the flexible load at the user determined location. At the given location, the RVM can be considered as a thrust generator along the sagittal plane. Thanks to the RVM design in II-B, the resultant thrust direction $\theta_{t,i}$ can be arbitrarily determined.

A. Flexibility Modeling of the Load

To model vibration of the flexible load, here, we adopt Euler-Bernoulli beams theory [13], whose governing equation is $\rho A \frac{\partial^2 w(x,t)}{\partial t^2} + \frac{\partial^2}{\partial x^2} EI \frac{\partial^2 w(x,t)}{\partial x^2} = 0$ where E, I, ρ, A are Young's modulus, the second moment of area, the density and the intersection area of the flexible load respectively.

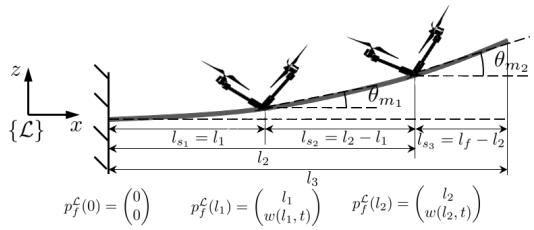

Fig. 3. Euler-Bernoulli beam deflection model.

We assume the constant parameters along the flexible load to simplify the beam model and to meet the practical objects. Using the separation of variables, a solution of given partial differential Euler-Bernoulli equation can be written s.t. $w(x,t) = \sum_{i=1}^{m} \phi_i(x)\delta_i(t) =: \Phi(x)\delta(t)$ where m is the number of assumed vibration modes, $\phi_i(x)$ is the time invariant mode shape function, $\delta_i(t)$ describes the time varying part of the deflection associated with given mode shape $\phi_i(x)$, $\Phi := [\phi_1, \cdots, \phi_m] \in \Re^m$ and $\delta := [\delta_1; \cdots; \delta_m] \in \Re^m$ are the corresponding row and column vector. In practice, high frequency modes are suppressed quickly due to their damping. thus, finite dimension m of the vibration modes are considered.

The attached location of the RVM can be arbitrarily chosen by the user, therefore, the flexible load model should be derived to adopt arbitrary number of the RVM system at arbitrary location. Since each RVM is rigidly attached to flexible beam, RVM provides substantial mass and moment of inertia at attached location. Therefore, to solve Euler-Bernoulli equation, the mass and the moment of inertia of each RVM should also be incorporated in the boundary condition: $M_{s_{i-1}}(l_{s_{i-1}}) = M_{s_i}(0) + \mathcal{I}_{m,i} \left.\frac{\partial \ddot{w}_s}{\partial x}\right|_{x=0}$ and $V_{s_{i-1}}(l_{s_{i-1}}) = -m_{m,i}\ddot{w}_s(0) + V_{s_i}(0)$ where $M(x) = E\frac{\partial^2 w}{\partial x^2}$ is the moment and $V(x) = -EI\frac{\partial^3 w}{\partial x^3}$ is the shear force and the subscript s_i represent i-th segments divided by $(i-1)$-th and i-th module with $l_0 = 0$ and $l_{n_m+1} = l_f$ as illustrated in Fig. 2 and Fig. 3. Therefore, the flexible load is divided into $n_m + 1$ segments. Since the length of the RVM module ($l \approx 0.05m$) is typically smaller than the length of manipulated flexible beam ($l_f > 1m$), the RVM location is approximately expressed as a point along x-axis. Then, the solution can be computed by simultaneously solving the Euler-Bernoulli equation of all segments. Note that the resultant mode shapes of all the segments are the eigenfunctions of the Euler-Bernoulli equation, thus the integration along the overall length still hold orthogonality between each mode shape for $i \neq j$ s.t.:

$$\int_0^{l_f} \phi_{ij}''(x)dx = 0 \tag{5}$$
$$\rho A \int_0^{l_f} \phi_{ij}(x)dx + \sum_{k=1}^{n_m} \left(m_{m,k}\phi_{ij}(l_k) + \mathcal{I}_{m,k}\phi_{ij}'(l_k) \right) = 0$$

where $\phi_{ij} := \phi_i\phi_j$ and $m_{m,i}$, $\mathcal{I}_{m,i}$ are mass and moment of inertia of i-th RVM.

As a result, we define the system configuration as $q = [\theta^T, \delta^T]^T \in \Re^{n+m}$ where $\delta \in \Re^m$ is the time-dependant deflection variable for the flexible load.

B. Euler-Lagrange Dynamics

Using the kinetic energy T and the potential energy U, the Lagrangian is defined as $L = T - U$. This Lagrangian is identical with standard robot except for the flexible load. To compute its kinetic energy, the position and velocity along the flexible load is necessary w.r.t. $\mathcal{W}$:

$$p_f(x) = p_e + R_{\mathcal{L}}^{\mathcal{W}} \left(x \;\; w(x,t)\right)^T, \quad \dot{p}_f(x) = J_f(x)\dot{q} \tag{6}$$

where $J_f \in \Re^{2\times(n+m)}$ is the flexible load Jacobian attached on robot arm, $1_m \in \Re^m$ is one vector, $e_2 = [0;1] \in \Re^2$ is the unit vector. Its corresponding kinetic energy is given as $T_{bar} = \frac{\rho A}{2}\int_0^{l_f} \dot{p}_f(x)^T \dot{p}_f(x)dx$.

Regarding the potential energy, the elastic energy is also different with standard robot dynamics $U_{bar,el} = \frac{EI}{2}\int_0^{l_b} \left(\frac{\partial^2 w}{\partial x^2}\right)^2 dx = \frac{EI}{2}\sum_{i=1}^m \sum_{j=1}^m d_{ij}\delta_i\delta_j$ where $d_{ij} := \int_0^{l_b} \phi_i''\phi_j''dx$ satisfies the orthogonality in (5).

Then, we can derive following Euler-Lagrange dynamics of the cooperative manipulation system with the RVM:

$$\begin{bmatrix} M_\theta & M_{\theta\delta} \\ M_{\delta\theta} & M_\delta \end{bmatrix} \ddot{q} + \begin{bmatrix} C_\theta & C_{\theta\delta} \\ C_{\delta\theta} & 0 \end{bmatrix} \dot{q} + g + \begin{bmatrix} 0 & 0 \\ 0 & K \end{bmatrix} q = B\tau \tag{7}$$

where $M_\theta \in \Re^{n\times n}$, $M_\delta \in \Re^{m\times m}$, $M_{\theta\delta} = M_{\delta\theta}^T \in \Re^{n\times m}$ are the inertia matrix, $C_\theta \in \Re^{n\times n}$, $C_{\delta\theta} \in \Re^{m\times n}$, $C_{\theta\delta} \in \Re^{n\times m}$ are the Corilois matrix, $g \in \Re^{n+m}$ is the gravity force vector, $B(q) \in \Re^{(n+m)\times(n+2n_m)}$ is the input mapping matrix, $\tau = [\tau_a; \tau_m] \in \Re^{n+m}$ is control input with the joint torque of manipulator $\tau_a \in \Re^n$ and the module thrust input $\tau_m = [\lambda_1 R_{m,1}e_2; \cdots; \lambda_{n_m} R_{m,n_m}e_2] \in \Re^{2n_m}$ where $R_{m,i} \in SO(2)$ is the rotation matrix of i-th module, and $\lambda_{m,i} \in \Re$ is the thrust magnitude. It is important to note that the inertia matrix for flexibility M_δ and the stiffness matrix K are constant diagonal matrix, even if multiple RVM in contrast to a single quadrotor in [2], where the off-diagonal terms are eliminated because $\dot{\delta}_i\dot{\delta}_j$ terms in the kinetic energy and $\delta_i\delta_j$ terms in the elastic energy meets the orthogonality properties (5). Note that the RVM is rigidly attached to the flexible load, thus its equation of motion is incorporated in the above dynamics. The input mapping matrix $B(q)$ have the following structure

$$B = \begin{bmatrix} I_n & B_{\theta m} \\ 0 & B_{\delta m} \end{bmatrix} \in \Re^{(n+m)\times(n+2n_m)}$$

where $I_n \in \Re^{n\times n}$ is the identity matrix, $B_{\theta m} = [J_{f\theta}^T(l_1) \cdots, J_{f\theta}^T(l_{n_m})] \in \Re^{n\times n_m}$ is the input mapping matrix from the module thrust to robot arm joints, $B_{\delta m} = [B_{\delta m,1} \cdots B_{\delta m,n_m}] \in \Re^{m\times 2n_m}$ is the input matrix for the flexibility dynamics with

$$B_{\delta m,i} = \Phi(l_i)^T[-\sin\bar{\theta}_l, \;\; \cos\bar{\theta}_l] \tag{8}$$

where $\bar{\theta}_l = \sum \theta_i + \theta_l$ is the absolute orientation of the flexible load at the end-effector of the arm. Note that the manipulator control input τ_a cannot directly apply its torque to the flexible load dynamics while the RVM input τ_m directly control the flexible load along $B_{\delta m}$. Since the matrix $B_{\delta m,i}$ has rank one although each RVM can generate thrust in $E(2)$, the m-dof flexible load dynamics can be under-actuated when the number of the RVM is less than the number of the mode shape (i.e., $n_m < m$).

IV. Controllability, Optimal Placement and Control Design

The controller design is motivated by diagonal and constant dynamic structure of the flexible load in (7). Then, we divide the control framework into the following two sub-problems: 1) fully-actuated robot arm nominal trajectory tracking; 2) flexible load vibration suppression and gravity compensation via the distributed RVMs.

However, as shown in the structure of $B_{\delta m}$ in (8), depending on the relation between the number of the modules n_m and mode shapes m, given robotic system can be under-actuated to the vibration dynamics. Thus, we analyse the controllability condition, which is only handled for single quadrotor attached on the flexible load in [2], therefore, the theory should be extended to distributed RVMs. In addition, the terms in $B_{\delta m}$ is determined by location of the RVMs, thus we can expect that the distribution of RVMs affect to not only controllability but also the control performance.

A. Flexible Load Dynamics Linearization

The fully actuated robot arm control guarantees $\xi \to \xi^d$ where $\xi = (p_e, \theta_e) \in \Re^3$ is end-effector pose. Therefore, the vibration dynamics can then be rewritten with ξ^d as follows

$$\begin{bmatrix} \ddot{\delta} \\ \dot{\delta} \end{bmatrix} = \begin{bmatrix} 0_m & -\bar{K} \\ I_m & 0_m \end{bmatrix} \begin{bmatrix} \dot{\delta} \\ \delta \end{bmatrix} + \begin{bmatrix} \bar{B}_{\delta m} \\ 0 \end{bmatrix} \tau_m - \begin{bmatrix} M_\delta^{-1} E \\ 0 \end{bmatrix} \tag{9}$$

where $\bar{K} := M_\delta^{-1} K$, $\bar{B}_{\delta m} := M_\delta^{-1} B_{\delta m}$ and E is defined as $E := M_{\delta\xi}\ddot{\xi}^d + C_{\delta\xi}\dot{\xi}^d + g_\delta(\bar{\theta}_e^d)$. We can further simplify the control input expression using the definition of $B_{\delta m}$ in (8) and τ_m as following

$$\bar{B}_{\delta,m}\tau_m = \underbrace{M_\delta^{-1}\left[\Phi(l_1)^T \cos\theta_{t,1}^{\mathcal{L}} \cdots \Phi(l_{n_m})^T \cos\theta_{t,n_m}^{\mathcal{L}}\right]}_{=:b_{\delta m} \in \Re^{m \times n_m}} \lambda_m$$

where $\theta_{t,i}^{\mathcal{L}} = \theta_{t,i} - \bar{\theta}_l$ is the relative thrust generation direction of i-th RVM w.r.t. the flexible load frame $\mathcal{L}$. Recall that θ_t can be independently controlled thanks to arbitrary thrust generation capability of RVM in $E(2)$ as stated in Sec. II.

Depending on relation between n_m, m and placement of the RVM, the system can loose its controllability. Therefore, we design the flexible load vibration/deflection suppression controller based on controllability analysis. To analyse controllability, we linearize the dynamics (9) at the equilibrium deflection $\delta_e \in \Re^m$ along the end-effector trajectory ξ^d.

We aim that the flexible load behaves similar to the rigid body, thus the control objective of the RVM includes both the vibration suppression (i.e., $\dot{\delta} = 0$) and the deflection compensation $w(l_f) = 0$. For this, we design a feedforward control input to compensate the gravity at the equilibrium deflection δ_e to satisfy $w(l_f) = 0$ is $\lambda_m = (\Phi K^{-1} b_{\delta m})^\dagger \Phi K^{-1} g_\delta(\bar{\theta}_e^d)$ where $(\cdot)^\dagger$ is Moore-Penrose pseudo inverse. Here, we choose the λ_m solution that minimize overall energy consumption by minimizing in terms of thrust two-norm. Then, the corresponding equilibrium deflection shape mode vector satisfies $\delta_e = (-I + K^{-1} b_{\delta m}(\Phi K^{-1} b_{\delta m})^{-1}\Phi) K^{-1} g_\delta(\bar{\theta}_e^d)$. Note that the equilibrium deflection δ_e enforced by λ_m satisfies zero deflection at the load-tip, i.e., $w(l_f) = \Phi\delta_e = 0$.

Finally, we can linearize the dynamics (9) at the equilibrium deflection δ_e

$$\begin{bmatrix} \ddot{\tilde{\delta}} \\ \dot{\tilde{\delta}} \end{bmatrix} = \underbrace{\begin{bmatrix} 0_m & -\bar{K} \\ I_m & 0_m \end{bmatrix}}_{=:A} \begin{bmatrix} \dot{\tilde{\delta}} \\ \tilde{\delta} \end{bmatrix} + \underbrace{\begin{bmatrix} \bar{b}_{\delta m} \\ 0 \end{bmatrix}}_{=:B} \bar{\lambda}_m \tag{10}$$

where $\tilde{\delta} = \delta - \delta_e$ and $\bar{\lambda}_m = \lambda_m - (\Phi K^{-1} b_{\delta m})^\dagger \Phi K^{-1} g_\delta$.

B. Controllability

The linearized flexible load dynamics (10) is represented by $2m$-dof configurations $(\dot{\tilde{\delta}}, \tilde{\delta}) \in \Re^{2m}$ with n_m-dof RVM inputs via $B\lambda_m$. And the input mapping matrix B is a function of the module placement $\phi_i(l_j)$ and the thrust direction $\theta_{t,i}$. Therefore, we need to verify whether the input λ_m can suppress the vibration/deflection in the linearized system. For this, we utilize the controllability matrix $\mathcal{C} := [B \;\; AB \;\; \cdots \;\; A^{2m-1}B] \in \Re^{2m \times 2mn_m}$ of the linearized dynamics (10) which is computed as follows

$$\mathcal{C} = I_2 \otimes \underbrace{\left[\bar{b}_{\delta m} \quad -\bar{K} \quad \cdots \quad (-\bar{K})^{m-1}\bar{b}_{\delta m}\right]}_{=:\mathcal{C}_s \in \Re^{m \times mn_m}} \tag{11}$$

where $\otimes$ is Kronecker product. The linearized flexible load dynamics (10) is controllable, if the controllability matrix has full row rank. Since the left term of Kronecker product is identity matrix, to figure out the controllability condition, we need to check the full row rank condition of $\mathcal{C}_s$. However, the controllability matrix is not a square matrix for multiple RVM case, thus we cannot directly apply previous result by checking determinant, c.f. square matrix $\mathcal{C}_s \in \Re^{m \times m}$ in [2]. Since the full row rank condition for $\mathcal{C}_s$ is equivalent to $\det(\mathcal{C}_s\mathcal{C}_s^T) > 0$, we first evaluate it.

Lemma 1 *Consider the submatrix of the controllability matrix $\mathcal{C}_s$ of the linearized system* (10)*. Then the matrix $\mathcal{C}_s$ satisfies following properties:*

$$\mathcal{C}_s\mathcal{C}_s^T = \sum_{i=1}^{n_m} diag(\bar{b}_{i,1}, \cdots, \bar{b}_{i,m}) \mathcal{K}_m \mathcal{K}_m^T diag(\bar{b}_{i,1}, \cdots, \bar{b}_{i,m})$$

where $\mathcal{K}_m := [1_m, \bar{K}1_m, \cdots, \bar{K}^{m-1}1_m]$ and $\bar{b}_{i,j}$ is (i,j) component of $\bar{b}_{\delta m}$; and

$$det(\mathcal{C}_s\mathcal{C}_s^T) = \prod_{i=1}^{m}(\sum_{j=1}^{n_m} \bar{b}_{i,j}^2) \cdot \prod_{\substack{k=2 \\ 1 \le l < k}}^{m} w_{n,k-l}^2 + f(b_{\delta m}, \mathcal{K}_m) \tag{12}$$

where $w_{n,k-l} := w_{n,k} - w_{n,l}$ and $f(b_{\delta m}, \mathcal{K}_m)$ is residual function satisfying following inequality:

$$f(l, \theta_m) \ge -\prod_{i=1}^{m}(\sum_{j=1}^{n_m} \bar{b}_{i,j}^2) \cdot \prod_{\substack{k=2 \\ 1 \le l < k}}^{m} w_{n,k-l}^2$$

where $\ge$ is replaced by $>$ only when $\prod_{i=1}^{m}(\sum_{j=1}^{n_m} \bar{b}_{i,j}^2) \cdot \prod_{\substack{k=2 \\ 1 \le l < k}}^{m} w_{n,k-l}^2 \neq 0$.

Proof: The first item is the result of straightforward calculation of the matrix multiplication. Regarding the second item, the given matrix $\mathcal{C}_s\mathcal{C}_s^T \in \Re^{m \times m}$ is positive semi-definite symmetric matrix and it always satisfy following inequality from $x\mathcal{C}_s\mathcal{C}_s^T x \ge 0, \forall x \in \Re^m : |x| = 1$ which is equivalent to $\det(\mathcal{C}_s\mathcal{C}_s^T) \ge 0$.

From the Leibniz formula of the matrix determinant, the determinant of $\mathcal{C}_s\mathcal{C}_s^T$ can be written as

$$\begin{aligned} \det(\mathcal{C}_s\mathcal{C}_s^T) = &\sum_{\sigma \in S_n} \operatorname{sgn}(\sigma) \prod_{i}^{n} \left((\sum_{j=1}^{n_m} \bar{b}_{i,j}\bar{b}_{\sigma_i,j}) \mathcal{K}_{m,1}\mathcal{K}_{m,\sigma_i}^T \right) \\ &\pm \prod_{i=1}^{m}(\sum_{j=1}^{n_m} \bar{b}_{i,j}^2) \sum_{\sigma \in S_n} \operatorname{sgn}(\sigma) \prod_{i}^{n} \left(\mathcal{K}_{m,1}\mathcal{K}_{m,\sigma_i}^T \right) \end{aligned} \tag{13}$$

where $\operatorname{sgn}(\cdot)$ is the sign function of permutations in the permutation group S_n which returns 1 or -1 for even and odd permutations respectively. We employ the result of Theorem 1 in [2] for $\det(\mathcal{K}_n)$ in second line equation which is similar to

well-known Vandermonde matrix structure whose determinant is given by

$$\det\left(\mathcal{K}_m\mathcal{K}_m^T\right) = \sum_{\sigma\in S_n}\text{sgn}(\sigma)\prod_{i}^{n}\left(\mathcal{K}_{m,1}\mathcal{K}_{m,\sigma_i}^T\right)$$
$$= \det\left(\mathcal{K}_m\right)^2 = \prod_{\substack{k=2\\1\le l<k}}^{m} w_{n,k-l}^2 \qquad (14)$$

Since this determinant is larger than zero and the term $(\sum_{j=1}^{n_m}\bar{b}_{i,j}^2) \geq 0$, the resultant product term in (12) and (13) should be larger than zero. This (14) explain the first term in (12) and the second line is equivalent with (13).

Other terms stand for the residual function $f(b_{\delta m}, \mathcal{K}_m)$. Regarding the residual function, if $\sum_{j=1}^{n_m}\bar{b}_{i,j}^2 \neq 0, \forall i = 1,\cdots,m$, then there exists i that satisfies $\text{diag}\left(\bar{b}_{i,1}\cdots,\bar{b}_{i,m}\right)x \neq 0, \forall x \in \Re^m : |x| = 1$. On the other hand, if $w_{n,i} \neq w_{n,j}, \forall i,j = 1,\cdots,m : i \neq j$, $\mathcal{K}_n\mathcal{K}_n^T$ is positive definite from its determinant expression in (14). If $\sum_{j=1}^{n_m}\bar{b}_{i,j}^2 = 0$ or $w_{n,k} = w_{n,l}$ for some i,j,l, then the inequality automatically hold due to semi-positive definite matrix $\mathcal{C}_s\mathcal{C}_s^T$. ∎

From Lemma 1, the three sufficient conditions to ensure controllability of the linearized system can be extracted in the following theorem:

Theorem 1 *Consider the linearized flexible load dynamics* (10) *and controllability matrix $\mathcal{C}$. Then, if the following three conditions are met, the linearized flexible load dynamics is controllable:*

1) ***Placing condition*** $\sum_{j=1}^{n_m}\phi_i(l_j)^2 \neq 0, \forall i = 1,\cdots,m$;
2) ***Tilting condition*** $\cos(\theta_{t,i}^{\mathcal{L}}) \neq 0$ *or* $\theta_{t,i}^{\mathcal{L}} \neq \frac{\pi}{2} + k\pi, k \in \mathcal{Z}$
3) ***Mode independency condition*** $w_{n,i} \neq w_{n,j}$.

Proof: According to Lemma 1, $\det(\mathcal{C}_s\mathcal{C}_s^T) > 0$ if $(\sum_{j=1}^{n_m}\bar{b}_{i,j}^2) \neq 0, \forall i = 1,\cdots,m$ and $w_{n,k-l}^2, \forall k,l = 1,\cdots,m$ and $k \neq l$. Therefore, the flexible load dynamics (10) is controllable when the placing, tilting and mode independency conditions meet. ∎

To satisfy the placing condition, at least one of the mode shape at the RVM location should not be zero for each vibration mode, i.e., $\sum_{j=1}^{n_m}\phi_i(l_j)^2 \neq 0, \forall i = 1,\cdots,m$. This controllability condition enforces a design criteria for attaching the RVM to avoid the node position, i.e., $\phi_i(x) = 0$. Unlike a single quadrotor case in previous result [2], even though one of the RVM is located at the node position of i-th mode, the whole system is controllable as long as there exists a RVM that are not located in node position of i-th mode.

If the RVM cannot meet the tilting condition, i.e., $\cos(\theta_{t,i}^{\mathcal{L}}) = 0$, then the thrust of the RVM is aligned to x-axis of the load frame $\mathcal{L}$ and subsequently cannot exert force along the deflection direction. This controllability condition impose to control the thrust direction to $\cos(\theta_{t,i}^{\mathcal{L}}) \neq 0$. This condition can always be preserved since the RVM is designed to instantly generate arbitrary direction thrust in the plane. On the other hand, If we use a quadrotor as shown in [2], the quadrotor attitude should be controlled to generate desired thrust direction.

Theorem 1 suggests sufficient conditions for the controllable system. The exact necessary and sufficient condition for controllability can elucidate when the system become uncontrollable, however, those exact conditions does not meet the practicality. For example, even though two vibration modes have same natural frequency against the physical condition, the system can be controllable with certain condition. However, the physical condition cannot be violated theoretically. Therefore, in practice, the sufficient conditions are enough to ensure controllability.

C. Optimal placement

In the previous section, the controllability is affected by how the RVMs are distributed along the flexible load. However, the controllability analysis does not explain how well the RVMs can suppress the vibration and what is the optimal RVM placement. For this, we adapt controllability gramian approach whose definition is given by $W_c = \int_0^\infty e^{A\tau}BB^Te^{A^T\tau}d\tau$. An asymptotically stable system should have unique bounded solution with integration along infinite time horizon. Since the linearized vibration dynamics is spring-mass system, we add the damping term to (10). This assumption is valid, because the real system always suppress the vibration with its own small damping as time goes by. The coefficient is verified to have small value $D \approx 0$, thus we add the diagonal damping term D similar to diagonal K, however, note that it can be neglected by assuming it to zero as we utilize in previous section.

Here, we transform the linearized dynamics (10) into equivalent state space representation to simplify controllability analysis as $\dot{x} = \hat{A}x + \hat{B}\lambda_m$ where $x = [\dot{\delta}_1; w_{n,1}\delta_1; \cdots, \dot{\delta}_m; w_{n,m}\delta_m] \in \Re^{2m}$ is transformed state and the matrix $\hat{A}$ and $\hat{B}$ satisfy corresponding transformation. Then, the controllability gramian solution is given in the following theorem

Theorem 2 *Consider the linearized flexible load dynamics $\dot{x} = \hat{A}x + \hat{B}\lambda_m$. Suppose the damping ratio satisfy $\zeta_i \ll w_{n,i}$ and $\zeta_i \approx 0, \forall i = 1,\cdots,m$. Then, the controllability gramian is derived s.t.,*

$$W_c \approx \textit{diag}(W_{11},\cdots,W_{mm}) \qquad (15)$$

where $W_{ii} = \textit{diag}\left(\frac{\beta_{ii}}{4\zeta_i w_{n,i}}, \frac{\beta_{ii}}{4\zeta_i w_{n,i}}\right)$ *and* $\beta_{ij} = \sum_{k=1}^{n_m}\bar{b}_{i,k}\bar{b}_{j,k}$.

Proof: Using transformed linearized dynamics, the controllability gramian can be solved by Sylvester equation similar to [14] and its block matrix is

$$W_{ij} = \frac{\beta_{ij}}{d_{ij}}\begin{bmatrix} a_{ij}(\zeta_i w_{n,j} + \zeta_j w_{n,i}) & w_{n,j}c_{ji} \\ -w_{n,i}c_{ji} & a_{ij}(\zeta_i w_{n,i} + \zeta_j w_{n,j}) \end{bmatrix}$$

with $d_{ij} = 4w_{n,i}w_{n,j}(\zeta_i w_{n,i} + \zeta_j w_{n,j})(\zeta_i w_{n,j} + \zeta_j w_{n,i}) + (w_{n,i}^2 - w_{n,j}^2)^2$, $a_{ij} = 2w_{n,i}w_{n,j}$ and $c_{ji} = (w_{n,j}^2 - w_{n,i}^2)$.

From the assumption $\zeta_i \ll w_{n,i}$ and $\zeta_i \approx 0$, $d_{ij} \approx (w_{n,i} - w_{n,j})^2$ for $i \neq j$ and $d_{ii} = 16w_{n,i}^3\zeta_i^2$ for $i = j$. Then, the off-diagonal block matrices are not depend on $1/\zeta$, however, the diagonal block matrices depend on $1/\zeta$. Therefore, the components in the off-diagonal matrices are approximated to zero since those are relatively smaller than the diagonal matrices in (15). ∎

Controllability gramian W_c characterizes the minimal energy required to steer the state from zero to certain state (i.e., $x^TW_c^{-1}x$) [15]. From this property, different quantitative measures of controllability considered in literature [16]. The

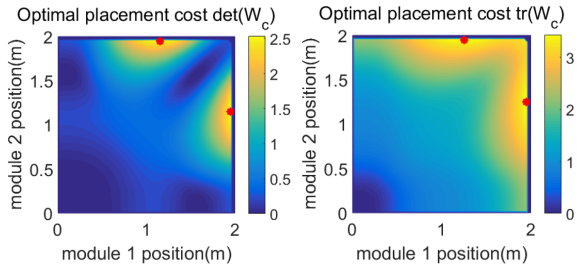

Fig. 4. Optimal placement of two RVMs on aluminum bar. $\det(W_c)$ provides $(l_1, l_2) = (1.15m, 1.95m)$ (left). $\mathrm{tr}(W_c)$ provides $(l_1, l_2) = (1.25m, 1.95m)$ (right).

trace of W_c related to the average control energy over random target states, however this metric cannot show how effectively it can suppress all the vibration, because only slow vibration modes are dominant. On the other hand, the determinant of W_c represents the volume of the ellipsoid containing the states that can be reached with an unit-energy, thus $\max \mathrm{tr}(W_c)$ represents the effectiveness of vibration suppression to every vibration modes. Here, we choose the controllability metric as the $\det(W_c)$ to effectively suppress the vibrations which is given in Fig. 4 for experimental setup in Sec. V. These metrics are represented by the singular values of W_c and directly computed by $\frac{\beta_{ii}}{4\zeta_i w_{n,i}}$ according to Theorem 2.

Theorem 2 gives an intuition that the location where it maximize mode deflection or its summation is the optimal placement which is compatible with Theorem 1 that shows the node positions can makes system uncontrollable. And the controllability conditions are also compatible with the structure of W_c in Theorem 2. In Theorem 2, the determinant of W_c is represented by the multiplication of the diagonal terms. The diagonal terms become zero when $\beta_{ii} = 0$ which is also shown in Lemma 1, thus W_c cannot be singular as long as placing and tilting condition hold.

D. Control Design

Here, we utilize LQR to optimally suppress vibration along with the gravity compensation for the RVM. And we utilize computed torque control for the robot arm. This control is same with the approach introduced in previous result. For more detail, please refer [2].

V. Experiment

We implement two RVMs attached on 2m long aluminium bar at optimal place in Fig. 4 with cross section $40mm \times 3mm$ as shown in Fig. 5. Each RVM is constructed based on optimal design in Sec. II and equipped with Pixhawk for computing, wireless communication between ground PC and ESCs control. MoCap is used to measure the position and orientation of each RVM and load-tip deflection. Power supply unit is used to supply power to the RVMs, however, each module can also be operated using onboard battery.

Two experimental verifications are performed for this two RVM system: 1) stationary robot arm with external disturbances and 2) one end position manipulated by robot arm. These two experiments are compared to the same scenarios without RVMs. In the first experiment, an operator exerts external disturbances every 3 to 5 seconds at various location on the aluminium bar. On the other hand, the disturbances are exerted every 9 to 10 seconds for the experiment without RVMs because the vibration persists for a long time. It takes about 1 min to totally suppress the vibration with its structural damping. The plot in Fig. 5

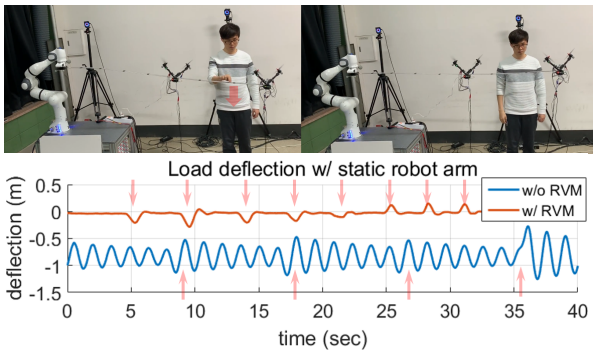

Fig. 5. Snapshots and load-tip deflection plot for stationary robot arm under external disturbances. Red arrows represent times external forces exerted.

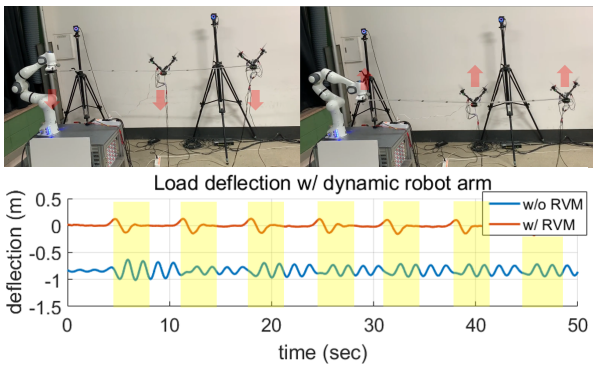

Fig. 6. Snapshots and load-tip deflection plot for one-end position manipulated by robot arm. Yellow shaded columns represent times the robot arm moves.

shows that RVMs effectively suppress the vibration before it reaches next peak of sinusoidal deflection.

In the second experiment, the external disturbances is replaced by the motion of robotic arm. To see the vibration suppression performance, the RVM input does not have feedforward input of the robot arm. The robot motion includes both upward and downward motion and this motion induces vibration. In Fig. 6, the plot shows that the RVM can suppress the vibration right after the motion stops. In contrast, without RVM, the plot shows that even though its amplitude is amplified or reduced depending on direction of robot arm motion and vibration, the vibration is not suppressed during the bar is manipulated.

Both two experiments also show that the gravity induced deflection of the aluminium bar is compensated by the RVMs so that the vibration shifted from -0.8m to 0m.

VI. Conclusion

We propose a novel RVM to manipulate and transport a large flexible object. The number of modules can be varied to adapt the various object since the RVM can be easily attachable/detachable. The RVM is optimally designed to maximize the feasible thrust generation area along the plane that vibration occurs with the minimum number of rotors while it minimizes undesirable torque. We derive the full dynamics of the distributed RVMs and elucidate the controllability condition. Furthermore, we also propose the optimal placement of the RVMs on the flexible load based on the controllability gramian. Experimental validation of the distributed RVMs is also presented. Some possible future research topics include: 1) sensor fusion with onboard sensor; 2) MoCap-less operation of distributed RVMs.

REFERENCES

[1] N. Staub, M. Mohammadi, D. Bicego, D. Prattichizzo, and A. Franchi. Towards robotic MAGMaS: Multiple aerial-ground manipulator systems. In *Proc. IEEE Int'l Conference on Robotics and Automation*, pages 1307–1312, 2017.

[2] H. Yang, N. Staub, A. Franchi, and D. J. Lee. Modeling and control of multiple aerial-ground manipulator system (magmas) with load flexibility. In *Proc. IEEE/RSJ Int'l Conference on Intelligent Robots and Systems*, pages 4840–4847, 2018.

[3] N. Staub, M. Mohammadi, D. Bicego, Q. Delamare, H. Yang, D. Prattichizzo, P. R. Giordano, D. J. Lee, and A. Franchi. The tele-magmas: An aerial-ground comanipulator system. *IEEE Robotics & Automation Magazine*, 25(4):66–75, 2018.

[4] A. Yamashita, T. Arai, J. Ota, and H. Asama. Motion planning of multiple mobile robots for cooperative manipulation and transportation. *IEEE Transactions on Robotics*, 19(2):223–237, 2003.

[5] Y. Hirata, Y. Kume, and T. Sawada. Handling of an object by multiple mobile manipulators in coordination based on caster-like dynamics. In *Proc. IEEE Int'l Conference on Robotics and Automation*, pages 807–812, 2004.

[6] D. Mellinger, M. Shomin, N. Michael, and V. Kumar. Cooperative grasping and transport using multiple quadrotors. In *Distributed Autonomous Robotic Systems*, pages 545–558, 2013.

[7] Gramazio Kohler Research. `http://www.gramaziokohler.arch.ethz.ch/web/e/forschung/index.html/`, Accessed: 2019-09-15.

[8] ATOUN. `http://atoun.co.jp/products/atoun-model-k/`, Accessed: 2019-09-15.

[9] R. Mahony, V. Kumar, and P. Corke. Multirotor Aerial Vehicles: Modeling, Estimation, and Control of Quadrotor. *IEEE Robotics & Automation Magazine*, 19(3):20–32, 2012.

[10] S. Park, J. Lee, J. Ahn, M. Kim, J. Her, G-H. Yang, and D. J. Lee. Odar: Aerial manipulation platform enabling omni-directional wrench generation. *IEEE/ASME Transactions on Mechatronic*, 23(4):1907–1918, 2018.

[11] H. Yang, S. Park, J. Lee, J. Ahn, D. Son, and D. J. Lee. Lasdra: Large-size aerial skeleton system with distributed rotor actuation. In *Proc. IEEE Int'l Conference on Robotics and Automation*, pages 7017–7023, 2018.

[12] S. Park, Y. Lee, J. Heo, and D. J. Lee. Pose and posture estimation of aerial skeleton systems for outdoor flying. In *Proc. IEEE Int'l Conference on Robotics and Automation*, pages 704–710, 2019.

[13] D. J. Inman. *Engineering Vibration*. Pearson, 2008.

[14] A. Hać and L. Liu. Sensor and actuator location in motion control of flexible structures. *Journal of Sound and Vibration*, 167(2):239–261, 1993.

[15] C. T. Chen. *Linear System Theory and Design*. Oxford University Press, Inc., 1998.

[16] F. Pasqualetti, S. Zampieri, and F. Bullo. Controllability metrics, limitations and algorithms for complex networks. *IEEE Transactions on Network Systems*, 1(1):40–52, 2014.